Photovoltaic Power Matching

Leander Merbecks
Find this project on GitHub

Introduction

In this document the optimization of a photovoltaic system is described. The motivation for the project is that while PV power systems have become readily available lately their power output is strictly bounded to the irradiance of the individual panels and modules. This leads to a power production characteristic that is not constant but varies over time. The characteristics shape over time depends heavily on the orientation of the PV panel as well as other secondary factors like shadows, weather and temperature [1]. Similar to the unsteady characteristic of the PV power system the power demand characteristic of residential homes is also non stationary. There is, however, little influence one can take on the shape of the demand characteristic of residential homes.

The similarity between the power production and power demand characteristics coupled with the possibility of changing one of the characteristics shape motivates the search for an optimal PV system with regards to power matching. I.e. the system whose power production characteristic matches the most with the power demand characteristic.

In the resulting optimization problem the main decision variables are the orientation of the PV panels that make up the PV power system. In this context orientation means both the tilt of the panel against the horizontal plane as well as the azimuth of the panel in the horizontal plane.

1. Modeling

To match the power characteristics of a photovoltaic system (PVS) to a power demand curve we first need to define a model that can compute these power characteristics based on driving design variables. Figure 1 shows the model structure schematically.

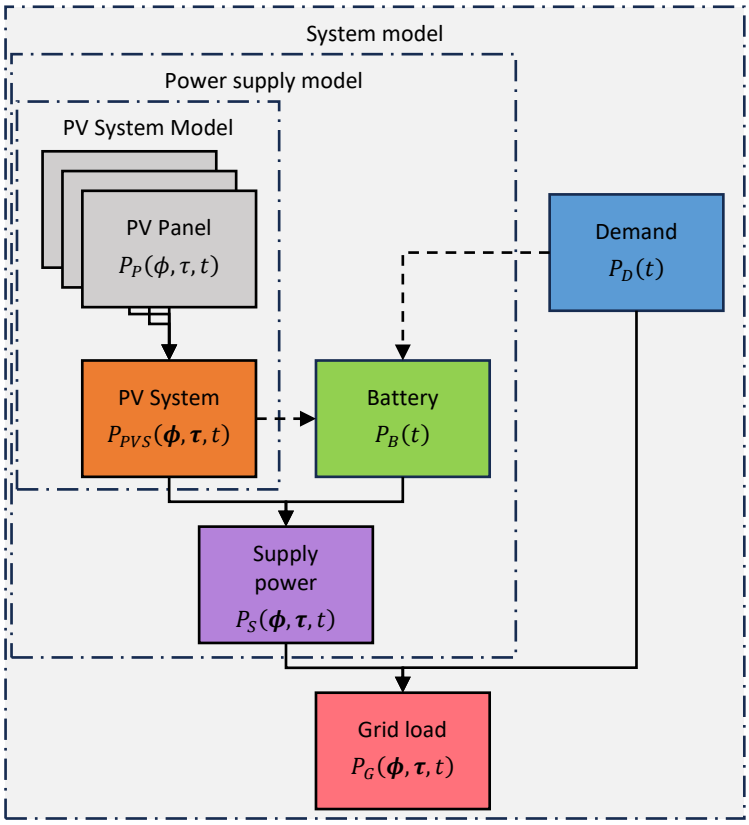

Figure 1: System model overview

In the Figure, solid arrows indicate the composition of components into a subsystem. Dashed arrows indicate relationships between components of the model. The (sub-)system boundaries are shown as dash-dotted lines.

For this project the goal is to match the power characteristics for a single day. The system is thus modeled for the fall equinox of 2024 at 22nd of September 2024. The equinox was chosen to keep computational demands low and obtain results that are closest to what is expected over a year.

The systems location on earth is also an important parameter. As the power demand data is based on real data the (approximate) location of the origin of that data is used. The location coordinates are given in Table 1.

Table 1: System location information

Variable	**Value**
Identifier	Essen, Germany
Latitude	$51.458069\ °N$
Longitude	$7.014761\ °E$
Elevation	$116.0\ m$

In the following Chapters the individual components of the system model are explained briefly and the driving equations are derived.

1.1. Demand model

The system model design starts with the power demand model as the power demand characteristic $P_D(t)$ dictates the behavior of other system components in the system model as indicated by the dashed arrows in Figure 1. The demand characteristic is derived from real world data that is shown in Figure 2.

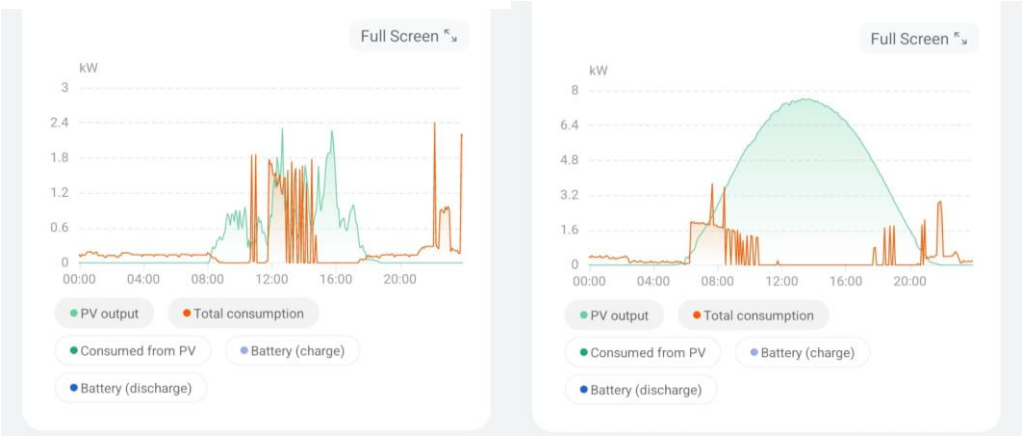

Figure 2: Reference data for the demand characteristics of a residential home.Source: Andreas Merbecks

There are two different characteristics available and they will be combined into a worst case demand characteristic. For this the data is first digitalized using the WebPlotDigitizer [2]. Subsequently the for each time of day the maximum of the two characteristics is taken to generate a worst case power demand characteristic. The resulting power demand characteristic of this residential home can be seen in Figure 3.

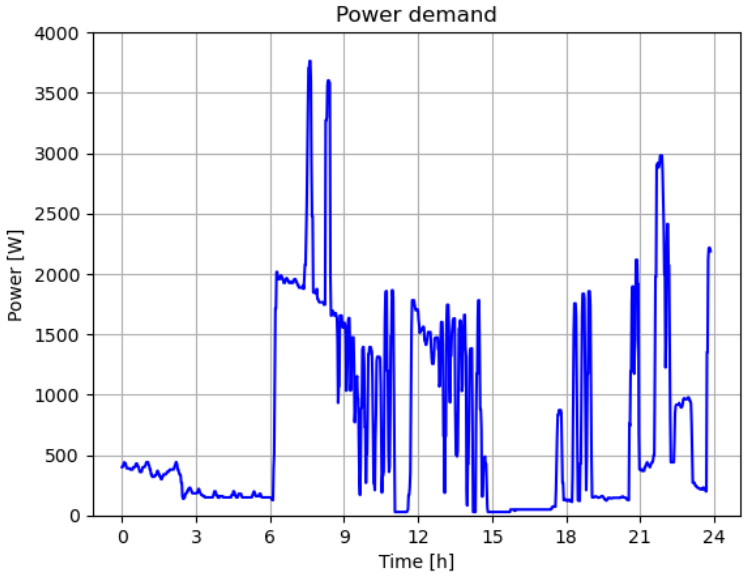

Figure 3: Power demand characteristic derived from real world data.

1.2. Photovoltaic panel model

In this project we model the power produced by a photovoltaic (PV) panel $P_{panel}(\phi, \tau, t)$ based on its orientation defined by the azimuth ϕ and the tilt angle τ. The two angles are shown in Figure 4 for a location on earth.

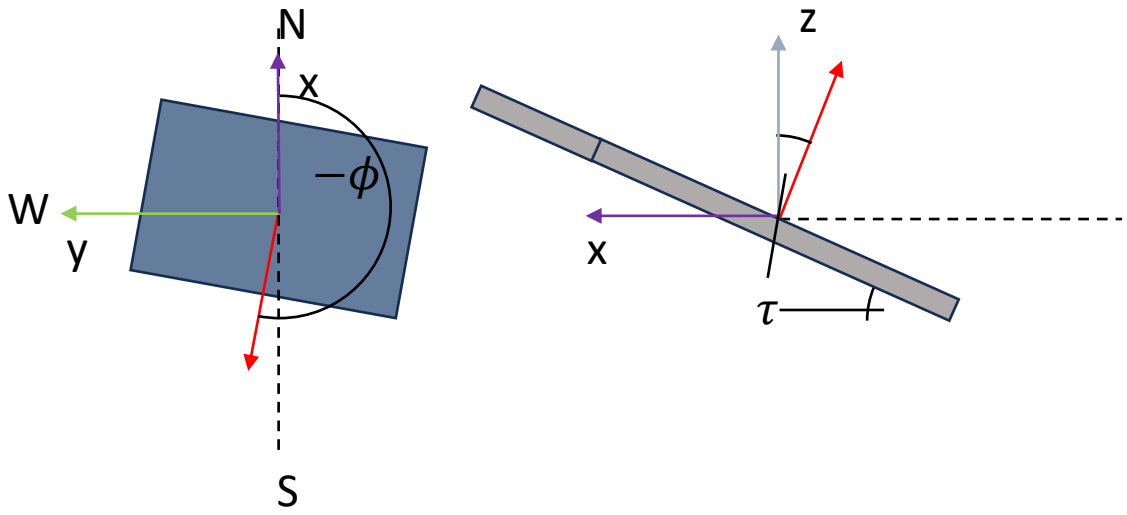

Figure 4: Tilt and azimuth of a PV panel, front panel surface normal in red.

As shown in Figure 4 a north west up (NWU) coordinate frame is used for all components in this project. This results in the azimuth of the panel to be mathematically negative explaining the sign in the Figure.

The power characteristic of the panel takes into account two influences. First the influence of angle of incidence and second the influence of atmospheric absorption. Both these influences are modeled as factors between zero and one that are multiplied with the maximum panel power:

$$P_{panel}(\phi, \tau, t) = P_{max} \cdot f_{\theta}(\phi, \tau, t) \cdot f_a(t)$$

The maximum panel power P_{max} denotes the power the panel produces if it lies flat on the ground and sunlight is shining perpendicular onto the front surface. In this project the maximum power is set to

$$P_{max} = 250W.$$

The factor $f_{\theta}(\phi, \tau, t)$ models the influence of the angle of incidence between the panels normal and the direction of incoming light. The atmospheric absorption is model using the factor $f_a(t)$.

The panel normal is needed to model the influence of the angle of incidence. Using the geometry in Figure 4 equations for the panel normal in the given NWU frame can be calculated as follows:

$$\vec{n}_{panel} = \left(x_{panel}, y_{panel}, z_{panel}\right)$$
$$x_{panel} = \sin\tau \cos -\phi$$

$$y_{panel} = \sin\tau \sin -\phi$$
$$z_{panel} = \cos\tau.$$

Per definition the panel normal is of length one. The sign of the azimuth is flipped to comply with the mathematical positive direction of angles. With this panel normal and other variables that are described in the following sections the influence factors can be defined.

1.2.1. Sun Model

For the influence factors described in the previous Chapter information on the suns position is needed as well. In this project this information is handled as a sun normal $\vec{n}_{sun}$ that points from the location of the system to the position of the sun in the sky above the system. The sun position in the sky is defined by the azimuth α and the elevation η. These two angles and the geometry of the sun position are defined in Figure 5. A NWU coordinate frame is used again which is why the sun azimuth has to be shown as negative.

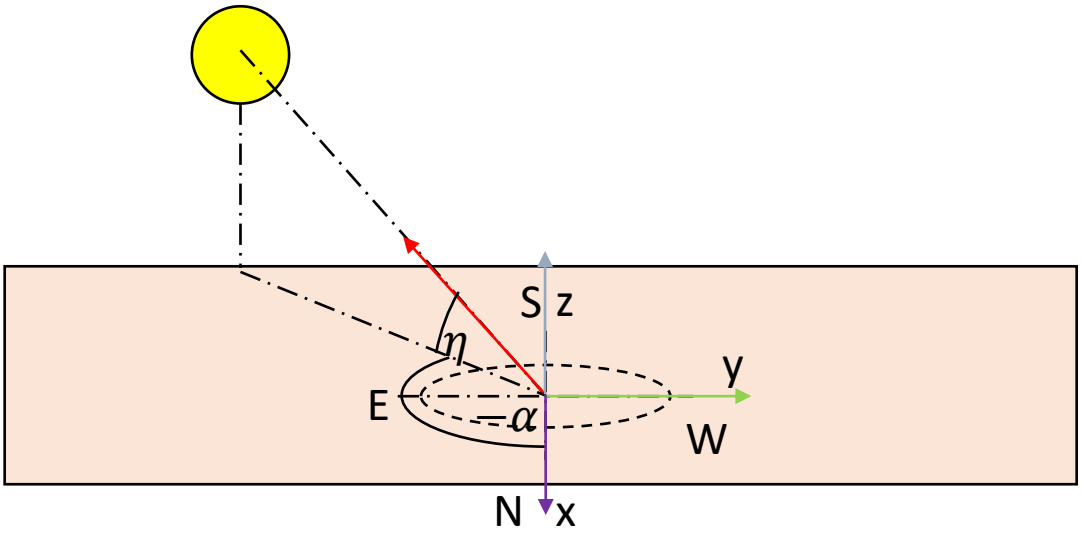

Figure 5: Angles for the sun position, sun normal in red.

The sun normal for a sun position in this coordinate frame can now be defined as follows:

$$\vec{n}_{sun} = (x_{sun}, y_{sun}, z_{sun})$$
$$x_{sun} = \sin(90° - \eta) \cos -\alpha$$
$$y_{sun} = \sin(90° - \eta) \sin -\alpha$$
$$z_{sun} = \cos(90° - \eta).$$

The sun does not stay at one position during the course of a day but travels along the sky. This means that the azimuth and the elevation and thus also the sun normal are time dependent. To model these time dependent sun normals ephemeris data is needed.

Astropy [3] [4] [5] is a python library that makes high precision ephemeris data available in python programs. Using this library the sun azimuth and elevation at any time can be determined for any location on earth. The angles for the fall equinox of 2024 at the system location from Table 1, are shown in Figure 6.

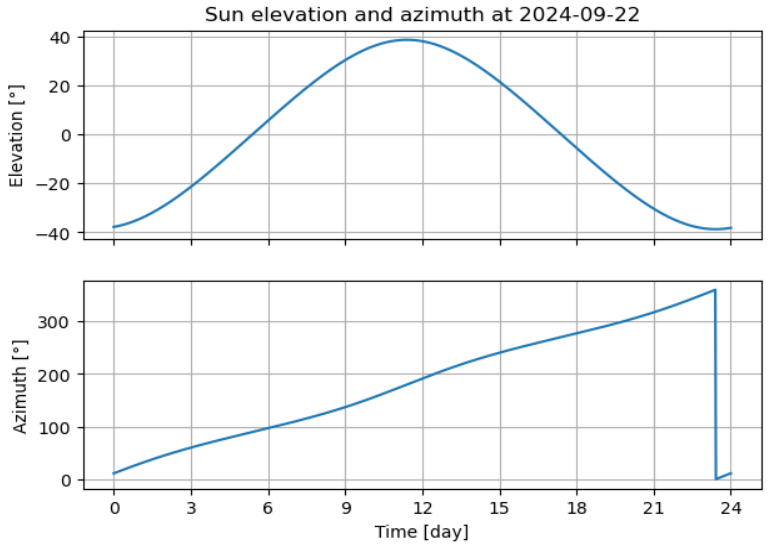

Figure 6: Azimuth and elevation at September equinox of 2024

With this data the sun normals are also defined in dependance of time:

$$\vec{n}_{sun}(t) = \vec{n}_{sun}(\alpha(t), \eta(t)$$

The time dependent sun normal for the fall equinox of 2024 are visualized in Figure 7. For reference a panel normal is also shown.

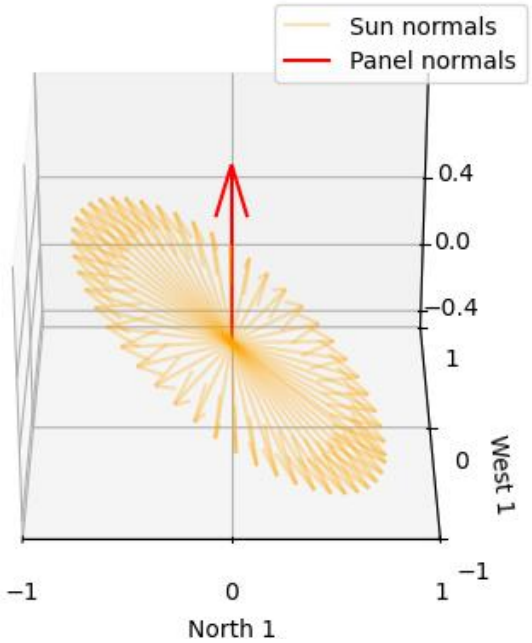

Figure 7: Time dependent sun normals in orange, panel normal in red.

The influence factors are defined in the following two chapters.

1.2.2. Angle of incidence influence

Firs the influence of the angle of incidence is modeled as factor f_θ. This influence factor assumes that the power of a panel P_{panel} is proportional to the projected surface A_p which

is the surface projected into the direction of the incoming sunlight. In other words the projected surface is the surface the sun rays "see" of the panel. The projected surface can be defined via the angle of incidence θ that is the angle between the panel normal and the direction of the sun light, i.e. the sun normal. This angle is shown in Figure 8.

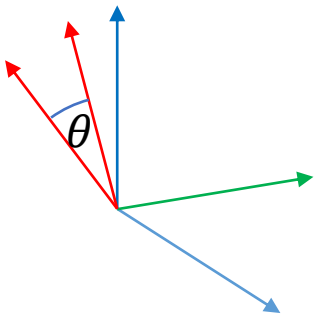

Figure 8: Angle of incidence between two normal vectors

With the angle of incidence the projected area can be calculated as follows [6]:

$$A_p = A \cdot \cos\theta.$$

As the maximum power of a panel was defined as the power for perpendicular sunlight for which the projected area is equal to the area A the influence factor is defined as follows:

$$f_\theta = \cos\theta$$

Using three dimensional algebra the cosine of the angle of incidence is given by:

$$\cos\theta = \frac{\vec{n}_{sun} \cdot \vec{n}_{panel}}{|\vec{n}_{sun}||\vec{n}_{panel}|} = \frac{\vec{n}_{sun} \cdot \vec{n}_{panel}}{\cancel{|\vec{n}_{sun}||\vec{n}_{panel}|}} = \vec{n}_{sun} \cdot \vec{n}_{panel}$$

In this $\cdot$ denotes the dot product. The fact that normal vectors are by definition of length one was used to simplify the equation. As the cosine of the angle of incidence is dependent on the panel orientation (ϕ, τ) and the sun normal $\vec{n}_{sun}(t)$ the influence factor is itself dependent on these variables:

$$f_\theta(\phi, \tau, t) = \vec{n}_{sun}(t) \cdot \vec{n}_{panel}(\phi, \tau)$$

1.2.3. Atmospheric influence

The second influence factor f_a models the influence of atmospheric transmittance. The model assumes that the transmittance is inversely proportional to the distance light has to travel through the atmosphere. This distance d_{ray} can be calculated using the elevation of the sun. The geometry for this is shown in Figure 9.

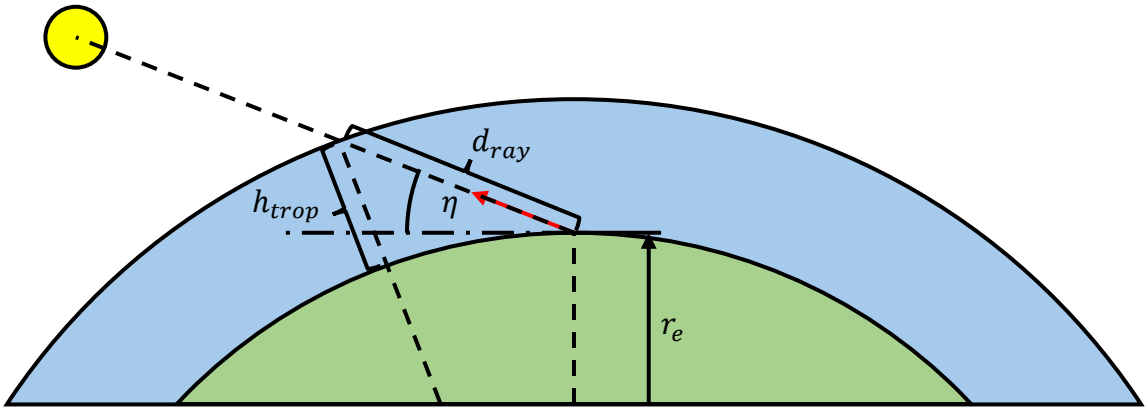

Figure 9: Atmospheric travel distance.

The assumption for this factor modeling is assumed that the troposphere is the only part of the atmosphere significantly impacting transmission of power. This is justified by the fact that the troposphere contains 80% of the atmospheres total mass. The height of the troposphere is varies from location to location on earth but is set to $h_{trop} = 20km$ in this project. [7]

Assuming that the earth is a sphere the cosine law can be used to describe the geometry:

$$\left(r_e + h_{trop}\right)^2 = r_e^2 + d_{ray}^2 - 2 \cdot d_{ray} \cdot r_e \cdot \cos(\eta + 90°)$$

This equation is a second degree polynomial in d_{ray} that can be solved analytically:

$$d_{ray} = -\frac{p}{2} + \sqrt{\left(\frac{p}{2}\right)^2 - q}$$
$$p = -2 \cdot r_e \cdot \cos(\eta + 90°)$$
$$q = r_e^2 - \left(r_e + h_{trop}\right)^2$$

The negative solution can be omitted in this case. It is now taken into consideration that the maximum power of a panel was defined for perpendicular illumination of a panel lying flat on the ground. This means that in this case the travel distance is equal to the height of the troposphere. Therefore, the influence factor f_a can be defined as:

$$f_a = \frac{h_{trop}}{d_{ray}}$$

As the travel distance is time dependent the absorption factor is time dependent as well:

$$f_a(t) = \frac{h_{trop}}{d_{ray}(t)}.$$

1.2.4. Panel model consolidation

Finally for the complete panel model all factors are combined. Additionally two conditions are added to prevent accurate power characteristics. The first condition is that the sun is above the horizon, i.e. $\eta(t) > 0°$, and the second condition is that the sun is in front of the panel, i.e. $\cos\theta\,(\phi, \tau, t) > 0$. With these conditions the panel power is defined as follows:

$$P_{panel}(\phi,\tau,t) = \begin{cases} P_{max} \cdot f_\theta(\phi,\tau,t) \cdot f_a(t), & if\ \eta(t) > 0° \wedge \cos\theta\,(\phi,\tau,t) > 0 \\ 0, & else \end{cases}$$

Examples of the power characteristics for two panels are shown in Figure 10.

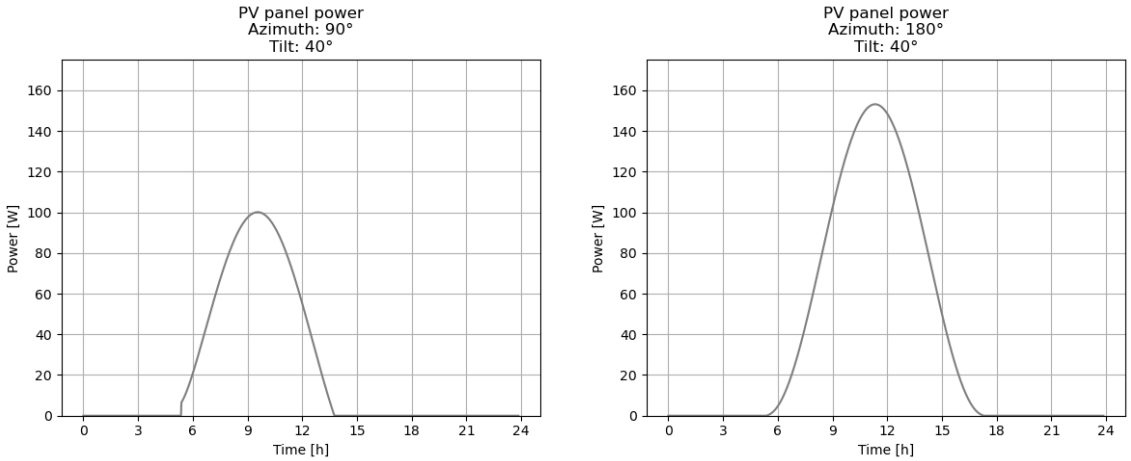

Figure 10: Panel power characteristics example

1.3. Photovoltaic system model

Now the power for each panel is defined and the power of the entire PVS can be described as the sum of all N individual panels in that system. The PVS power is dependent on the $1 \times N$ vectors for the panels azimuth and tilt angles $\boldsymbol{\phi}$ and $\boldsymbol{\tau}$ as well as the time.

$$P_{PVS}(\boldsymbol{\phi},\boldsymbol{\tau},t) = \sum_{i=1}^{N} P_{panel}(\phi_i,\tau_i,t)$$

Figure 11 shows an example of a power characteristic for a PVS.

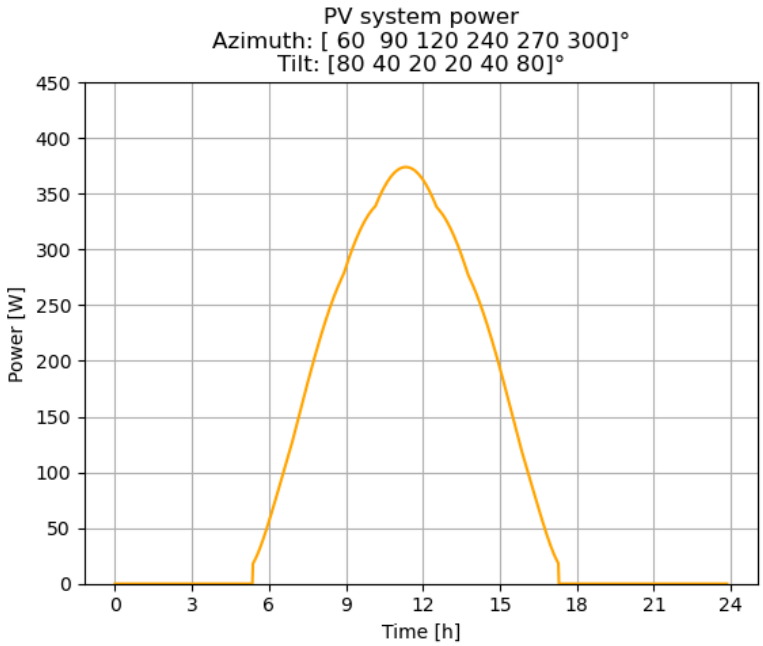

Figure 11: Photovoltaic system power characteristic.

1.4. Battery model

The battery serves as a way of storing power the PVS produces and providing it afterwards when needed. There are two parameters that define the battery: first the battery capacity $C_{B,max}$ and second the battery maximum power $P_{B,max}$ which is the maximum power the battery can be drained and charged at. Usually the drain and charging powers differ for batteries but for this simple model this was neglected. The properties of the battery used in this project are listed in Table 2.

Table 2: Properties of battery

Property	**Value**
Capacity $C_{B,max}$	$5\ kWh$
Maximum power $P_{B,max}$	$1kW$

To simulate the battery the demand characteristic and the PVS characteristic are subtracted from each other to form a combined power characteristic $P_C(t)$:

$$P_C(t) = P_D(t) - P_{PVS}(t)$$

Next, two characteristics are defined for the battery. First the battery charge $C_B(t)$ and second the battery power $P_B(t)$. The battery power is defined as positive when the battery is draining and negative if the battery is charging. Then for all M times in the time vector $\boldsymbol{t} = [t_1, t_2, \dots, t_i, \dots, t_M]$ with a uniform time step of Δt the battery charge and the battery power is calculated according to the following algorithm:

- If the combined power is $P_C(t_i) < 0$ the PVS supplies more power than demanded and the battery can be charged, provided the battery is not already full. First a potential power is defined:

  $$P_{pot} = \min(|P_C(t_i)|, P_{B,max})$$

  Here the minimum function ensures that the maximum charging power is less equal than the maximum battery power. Next a charge increment is defined

  $$\Delta C = P_{pot} \cdot \Delta t$$

  and the battery charge is calculated via:

  $$C_B(t_i) = \min(C_B(t_{i-1}), C_{B,max}).$$

  In this formula the minimum function enforces the capacity limit for the battery. For the battery power is defined based whether the capacity in the previous time step is less or greater equal to the battery capacity:

  $$P_B(t_i) = \begin{cases} -P_{pot}, & if\ C_B(t_{i-1}) < C_{B,max} \\ 0, & else \end{cases}$$

  The sign flip ensures compliance with the defined power directions.
- If the combined power is $P_C(t_i) > 0$ the PVS does not provide sufficient power to cover the demand and the battery max be drained, if it has charge to spare. Again, a potential power and *discharge* increment are defined:

  $$P_{pot} = \min\big(|P_C(t_i)|, P_{B,max}\big)$$
  $$\Delta C = P_{pot} \cdot \Delta t$$

  The battery power and the battery charge are now dependent on whether the charge of the battery in the previous time step is greater equal or less than the *discharge* increment:

$$C_B(t_i) = \begin{cases} C_B(t_{i-1}) - \Delta C, & if\ C_B(t_{i-1}) \geq \Delta C \\ C_B(t_{i-1}), & else \end{cases}$$
$$P_B(t_i) = \begin{cases} P_{pot}, & if\ C_B(t_{i-1}) \geq \Delta C \\ 0, & else \end{cases}$$

- If neither of the previous cases take place the PVS is matching the demand perfectly and the battery charge remains unchanged while the battery power is zero:

$$C_B(t_i) = C_B(t_{i-1})$$
$$P_B(t_i) = 0$$

With this algorithm the battery characteristic and the battery charge can be determined over the investigated time. An exemplary result of this algorithms can be seen in Figure 12. The combined power as decision variable is also plotted in this figure.

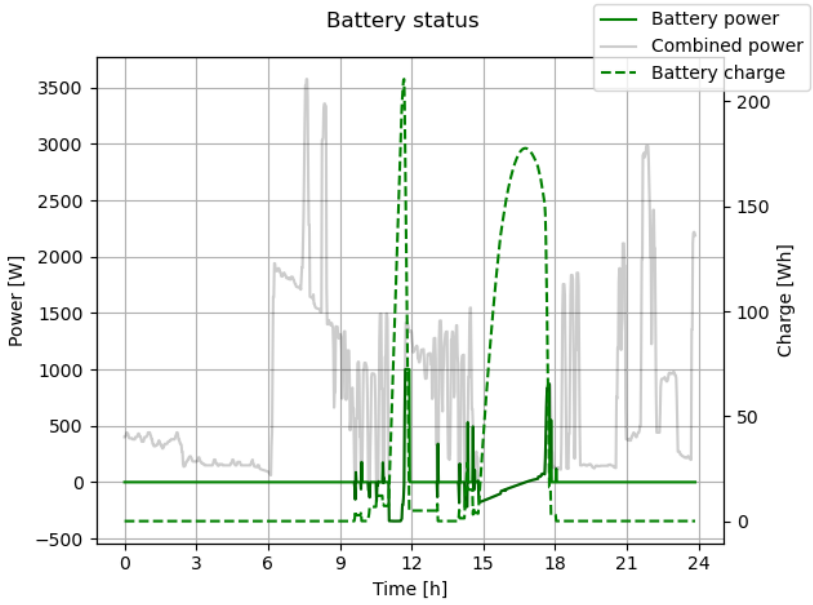

Figure 12: Battery status characteristics

1.5. Supply system model

The supply system model combines the PVS with the battery power to create a supply power characteristic $P_S(t)$ which is defined by:

$$P_S(\boldsymbol{\phi}, \boldsymbol{\tau}, t) = P_{PVS}(\boldsymbol{\phi}, \boldsymbol{\tau}, t) + P_S(t)$$

In other words this characteristic defines all the power of the PVS that does not go into charging the battery plus all power gained by draining the battery. A resulting characteristic for this is visualized in Figure 13.

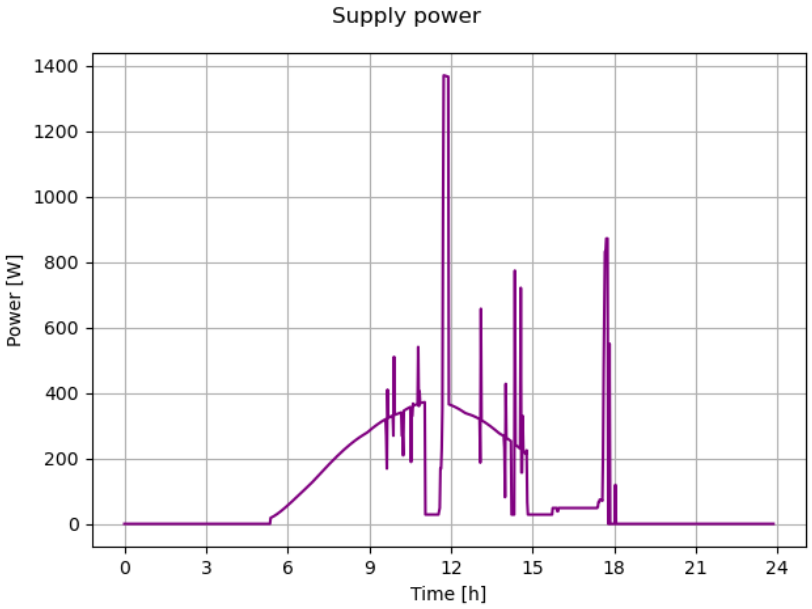

Figure 13: Supply power characteristic

1.6. Grid load model

This is the last step for the model. The supply power characteristic is subtracted from the demand characteristic to create a grid load characteristic $P_G(\boldsymbol{\phi}, \boldsymbol{\tau}, t)$ that represents how the power grid sees the load. Here positive powers mean that the grid is supplying power to the load and negative powers represent the load selling power to the grid.

$$P_G(\boldsymbol{\phi}, \boldsymbol{\tau}, t) = P_D(t) - P_S(\boldsymbol{\phi}, \boldsymbol{\tau}, t)$$

Figure 14 illustrates this characteristic. A time where the grid load sells power to the grid can be seen between 9:00 to 12:00 while the load buys power from the grid for the majority of the day.

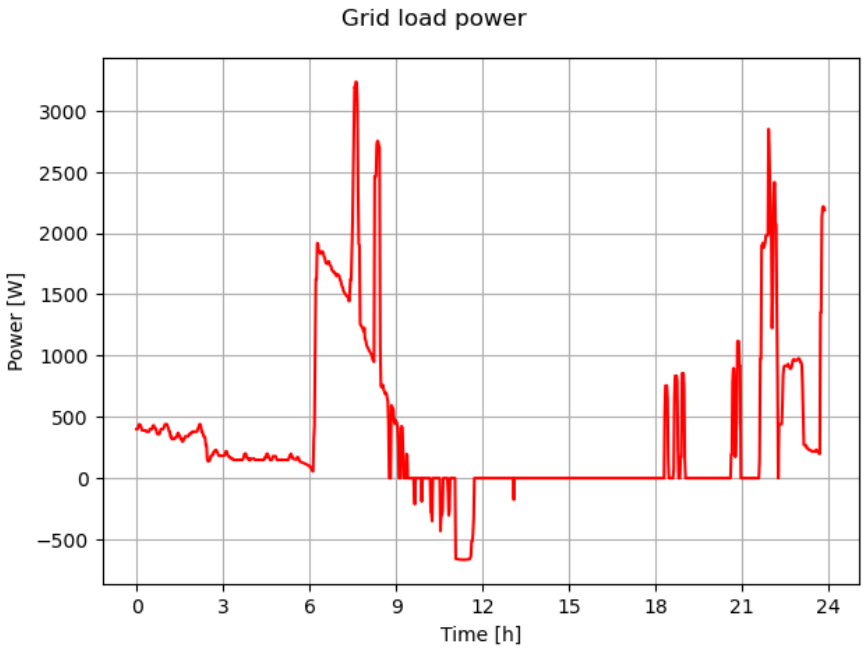

Figure 14: Grid load characteristic

2. Optimization

With the model completed the optimization can begin. In the next chapters the decision variables is presented, the objective function defined and the optimization algorithm described.

2.1. Objective function

The objective function for this project is the cost of electric energy for one day. This cost can be defined via the grid load characteristic and the cost of buying power from the grid c_e and the feed-in tariff for selling power to the grid p_e. As the system under investigation is located in Germany the corresponding values for this country are used. The values are listed in Table 3.

Table 3: Electricity costs and feed-in tariffs for Germany 2024

Parameter	**Value**
Electricity cost c_b	$0.41€/kWh$ [8]
Feed-in tariff p_e	$0.08€/kWh$ [9]

The cost of electricity can now be calculated by summing the grid load power characteristic:

$$C_e(\boldsymbol{\phi}, \boldsymbol{\tau}) = \sum_i P_G(\boldsymbol{\phi}, \boldsymbol{\tau}, t_i) \cdot \Delta t \cdot \begin{cases} c_e, & if\ P_G(\boldsymbol{\phi}, \boldsymbol{\tau}, t_i) > 0 \\ p_e, & if P_G(\boldsymbol{\phi}, \boldsymbol{\tau}, t_i) < 0 \end{cases}$$

The goal for the optimization is to minimize this cost.

2.2. Decision variables

As hinted at in the objective function, the decision variables are the azimuth and tilt angles of the N panels. These are $2N$ real variables. However, to let the optimization decide itself how many panels shall be used, another integer variable κ is introduced that can cut off as much as N panels from the system. In mathematical terms the integer variable extracts all first κ elements out of the set of N elements for both the azimuth and the tilt angle vectors.

All decision variables are subject to bounds that are listed in Table 4. The azimuth angles are bound by they angle of a full circle, preventing ambiguous panel azimuth angles. The bound on the tilt angles ensures panels are not pointed into the ground.

Table 4: Bounds for decision variables

Decision variable	**Lower bound**	**Upper bound**
$\boldsymbol{\phi}$	$\phi_i \geq 0° \; \forall \phi_i \in \boldsymbol{\phi}$	$\phi_i \leq 360° \; \forall \phi_i \in \boldsymbol{\phi}$
$\boldsymbol{\tau}$	$\tau_i \geq 0° \; \forall \tau_i \in \boldsymbol{\tau}$	$\tau_i \leq 90° \; \forall \tau_i \in \boldsymbol{\tau}$
κ	$\kappa \geq 0$	$\kappa \leq N$

2.3. Optimization algorithm

As the system model is non-linear and uses both integer as well as real decision variables a genetic algorithm was used to optimize the model. The optimized variables are the variables described in the previous chapter.

The genetic algorithm is an evolutionary optimization method that computes the objective function for individuals in a population. Here an individual is a set of the decision variables with a concrete value. The algorithm evaluates individuals in a population according to their objective function and passes the best individuals on to the next generation. Additionally, some individuals of the next generation combine to form new individuals in a process called crossover. As a last step the individuals are randomly mutated. The algorithm selected for this project uses tournament selection, heuristic crossover and random mutation [10].

The parameters for the genetic algorithm are listed in Table 5. Most of these variables are experience variables that were found through trial and error analysis, while others like the maximum number of panels are arbitrarily chosen as they would depend on the space constraints for the location of the PVS.

Table 5: Optimization algorithm parameters

Parameter	**Value**
Number of generations N_G	200
Individuals per population N_P	500
Tournament probability p_t	80%

Crossover probability p_{co}	80%
Mutation probability p_m	7.5%
Maximum number of panels N	20
Number of real variables per individual $2N$	40
Number of integer variables per individual	1

3. Results

In this chapter the results of the optimization are presented. There were two cases performed for both a system without a battery and a system with a battery. These cases were first a statistical run of the optimization algorithm for 100 times to eliminate potential optimization fails due to chance and validate the optimization results.

The second case runs optimizations on four possible future scenarios. As the feed-in tariff has continuously decreased since 2005, a possible scenario is that feed-in is not paid in the near future for small PVS [9]. An even worse scenario is that the feed-in tariff becomes negative, i.e. a fee has to be paid to be allowed to push power into the grid, a condition that has occurred on the German electricity market already. Additionally, the electricity cost in Germany has increased substantially over the course of the last decade [11]. These circumstances motivate optimization runs for four different scenarios that have different electricity costs and feed-in tariffs listed in Table 6.

Table 6: Scenarios with different feed-in tariffs and electricity costs.

Scenario	**Electricity cost** c_e $\left[\frac{€}{kWh}\right]$	**Feed-in tariff** p_e $\left[\frac{€}{kWh}\right]$
1	0.41	-0.10
2	0.41	0
3	0.55	-0.10
4	0.55	0

Due to computation limits no statistical runs were performed for these scenarios.

3.1. System without battery

The first results to be presented stem from a photovoltaic power supply system that does not include a battery.

3.1.1. Statistical Run

Figure 15 shows a histogram for the results of the statistical run. In this histogram a spread of the optimum values of approximately 0.25€ can be seen. Also, a bimodal distribution is visible with peaks at 3€ and 3.15€ justifying the statistical runs. Due to the peak for

3€ it can be said, however, that this is the best possible value for the system without a battery.

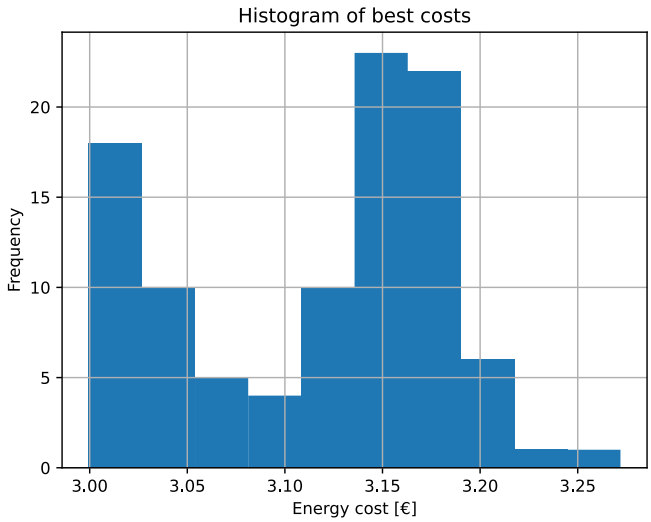

Figure 15: Histogram of best energy cost per day for model without battery

Figure 16 visualizes the progress of the optimization algorithm over the number of generations for the best result of the system without battery. The diagram shows that the optimal result is reached within the 200 generations and there are no significant changes in the objective function. Because the objective function decreases rather slow it could be argued that a higher number of generations could lead to better results. This could not be done in this project however, due to limited computational resources.

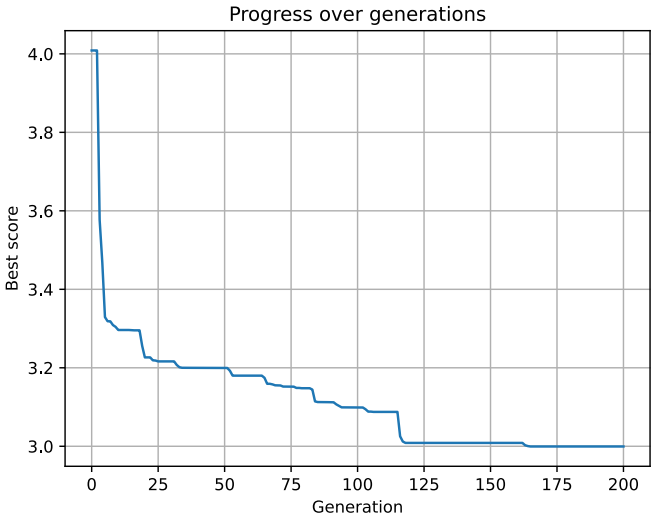

Figure 16: Optimization progress over generations for best result without battery

The optimal angles are listed in Table 7. The optimization algorithm determined that a total of 20 panels should be used for this scenario.

Table 7: Optimization results for system without battery.

Variable	**Value**
Azimuth angles ϕ [°]	[158, 157, 156, 151, 162, 149, 169, 160, 167, 167, 157, 152, 157, 167, 163, 155, 157, 151, 170, 160]
Tilt angles τ [°]	[52, 48, 34, 54, 47, 45, 57, 46, 35, 47, 60, 60, 53, 41, 51, 51, 50, 53, 52, 51]
Panels used	20
Electricity cost C_e [€]	3

Figure 17 shows the tilt and azimuth angles of the best run for a system without battery. It is clear from this histogram that the optimal azimuth angles for the panels are within $\phi_{opt} = [150°, 170°]$ and the optimal tilt angles are within $\tau_{opt} = [40°, 60°]$.

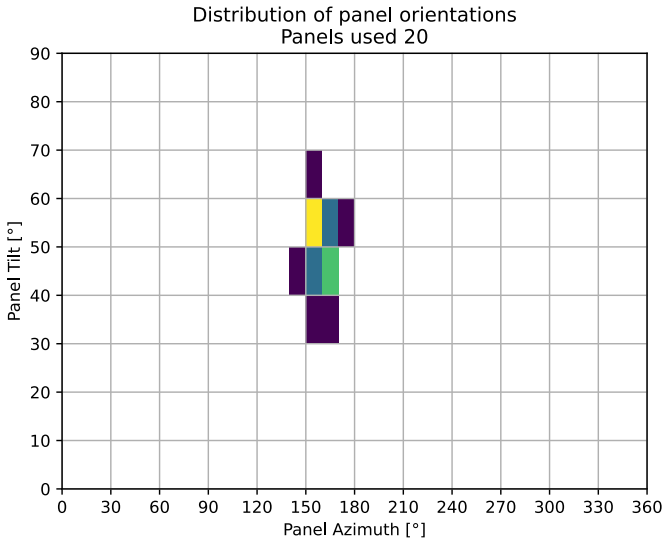

Figure 17: Histogram of panel orientations for best result from statistical run without battery.

Figure 18 shows the power characteristics for the best result for a system without a battery. Interestingly, against the original hypothesis and motivation of this project a clear matching of the PVS characteristic to the demand power cannot be seen clearly. However, it can be seen that the power maximum is shifted slightly to the morning, where a lot of power is demanded. So the characteristics were matched slightly for this time of day.

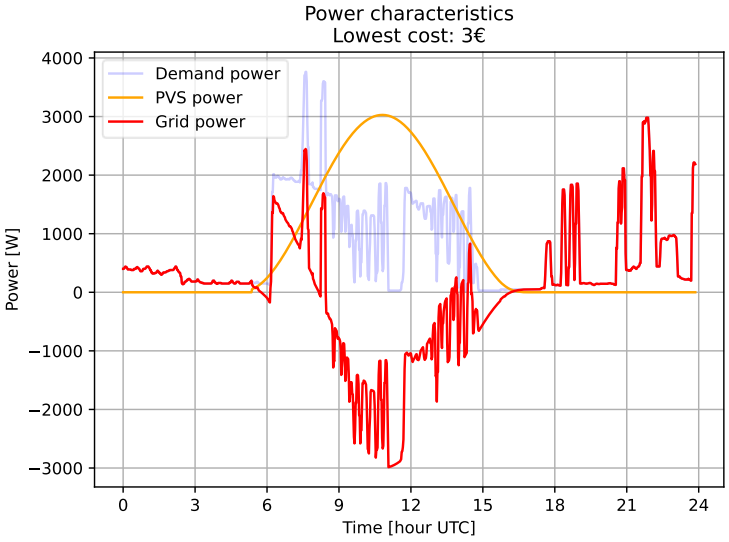

Figure 18: Power characteristics for best result from statistical run without battery.

Interpreting the results further, it seems logical that the power characteristics are not matched precisely. A possible reason is that the feeding of power into the grid is not penalized but actually encouraged. Therefore, the optimization tries to maximize the power generated by the PV system instead of matching it to the power demand. This is another motivation for the future scenario runs.

3.1.2. Future Scenarios Run

The results for the future scenario runs are shown in Figure 19 as histograms of the panel orientation and in Figure 20 as the power characteristics for the scenarios.

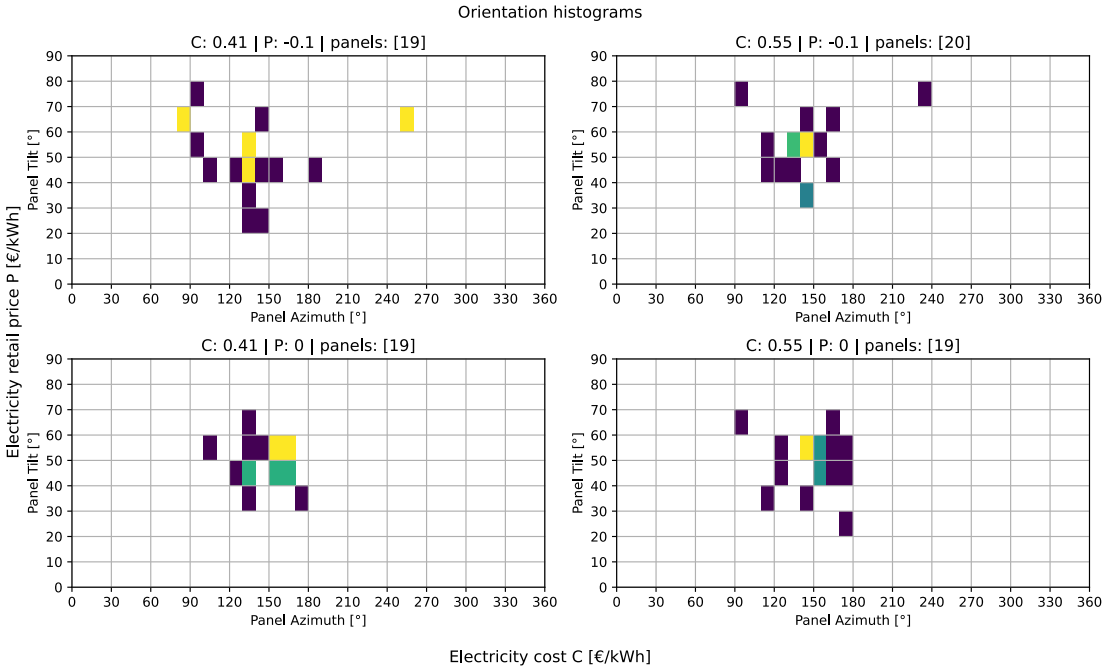

Figure 19: Histograms of angles for different electricity costs and feed-in tariffs

For the panel orientations it is obvious that the orientations spread a lot more than the result for the statistical runs. This can imply that the number of generations is too small and the algorithm would need more time to make the result more precise. For electricity costs similar to those for today but a negative feed-in tariff the orientations drift apart and for the first time in this project glimpses of power matching can be observed, as the optimization orients panels significantly more to the east and also a few to the west. This generates a power characteristic that is shifted more to the morning but has lower maximum power as seen in Figure 20.

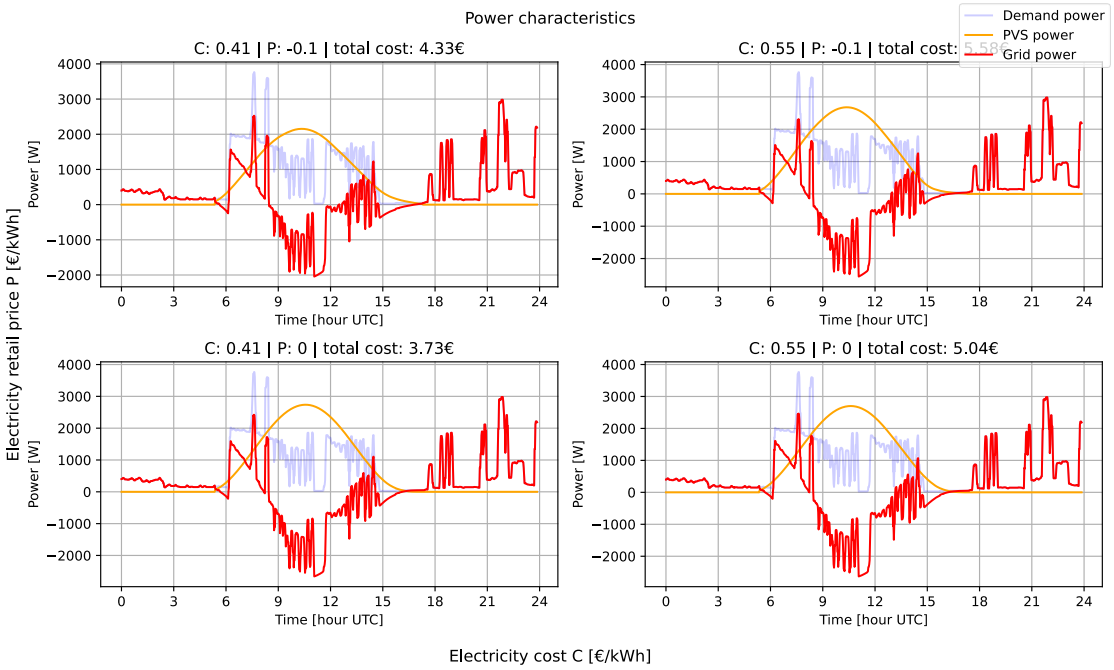

Figure 20: Power characteristics for different electricity costs and feed-in tariffs

The power characteristics for all further scenarios seem to be almost indifferent to the optimal result obtained from the previous section except the maximum power of the PV system was significantly decreased. It can also be observed that the optimization algorithm chose to reduce the number of panels from 20 to 19 in three cases, indicating that overproviding power is sought to be avoided for these scenarios.

3.2. System with battery

Next the results for a system with battery are presented and interpreted.

3.2.1. Statistical Run

Figure 21 shows a histogram of resulting electricity costs for the statistical run. A maximum is visible for the 1.95€ and the spread is around 0.25€ similar to the spread for the system without a battery. Thus, it seems the optimization algorithm works as expected and the optimal result should be a true optimum for the system. Unlike for the system with no battery this histogram shows no signs of two maxima.

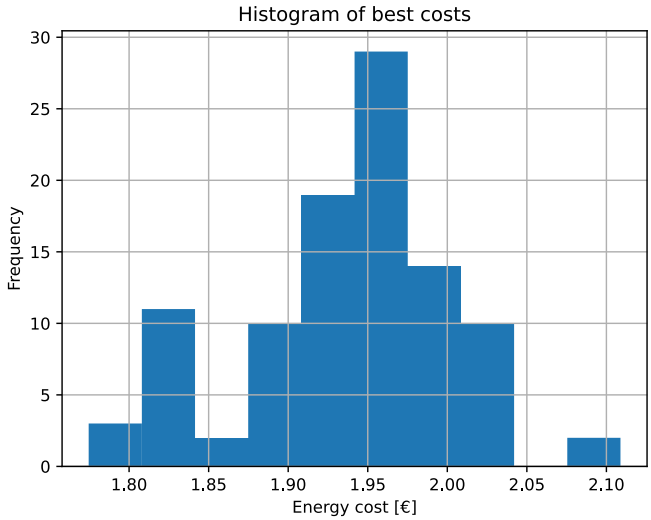

Figure 21: Histogram of statistical run for system with battery.

The progress of the optimization over generations for the best result is illustrated in Figure 22. After the 100th generation the optimal result does not seem to change much but some improvements are made close to the 200th generation. An increase of the generation limit to a number over 200 could, thus, yield better results but would increase the computational effort. It was decided that this additional effort does not justify the marginal improvements to the optimization results.

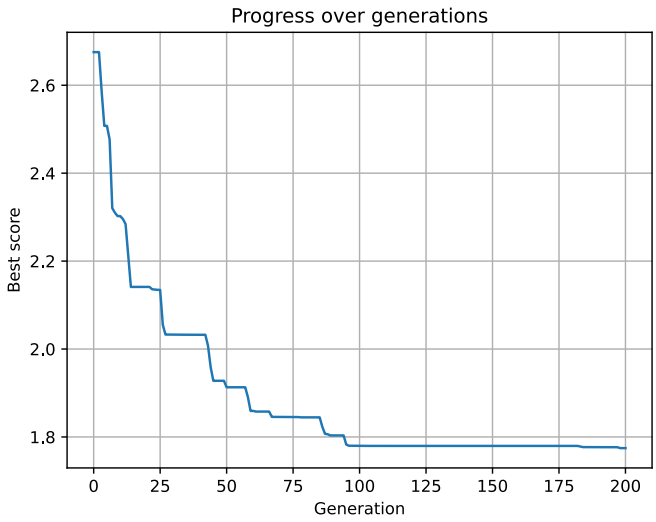

Figure 22: Progress over generations for best result of system with battery.

The optimization results for the system with a battery are listed in Table 8.

Table 8: Optimization results for system with battery

Variable	**Value**
Azimuth angles ϕ [°]	[132, 135, 134,154, 132, 135, 152, 154, 134, 133,

	126, 133, 127, 138, 144, 144, 141, 135, 142, 140]
Tilt angles τ [°]	[48, 54, 53, 43, 56, 47, 65, 45, 52, 50, 51, 61, 52, 41, 53 48, 61, 50, 49, 57]
Panels used	20
Electricity cost C_e [€]	1.77

Figure 23 visualizes the optimization results for the panel orientations. It appears that the panel orientations spread only very little and center around a azimuth range of $\phi \in [130°,\ 140°]$ and a tilt range of $\tau \in [50°, 60°]$. The orientation is a bit east biased which could be explained by the high power demand in the morning.

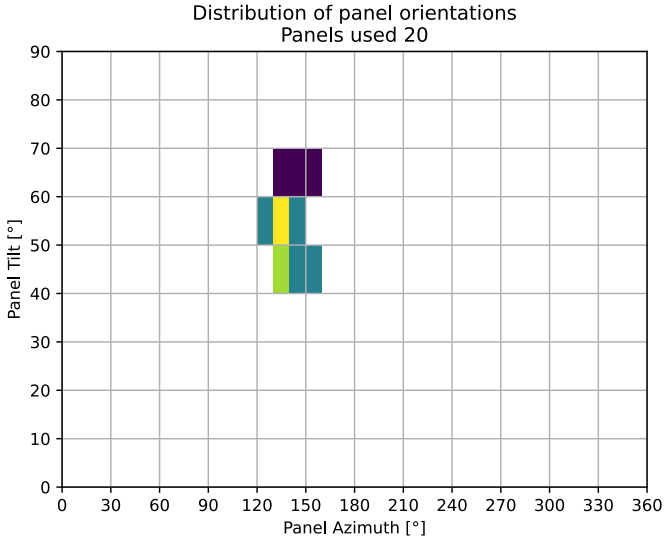

Figure 23: Histogram of panel orientations for system with battery

More insight into the reasons behind the panel orientations is obtainable by plotting the power characteristics for the problem as in Figure 24. It becomes apparent while analyzing these characteristics that the PVS characteristic is shifted to the morning but the maximum output is still close to noon. In comparison with the system without a battery the characteristic is shifted about one hour more to the morning. Seemingly the optimization algorithm tries to charge the battery as much as possible during the morning hours in the period with low demand. The battery can then cover the demand almost completely for the evening.

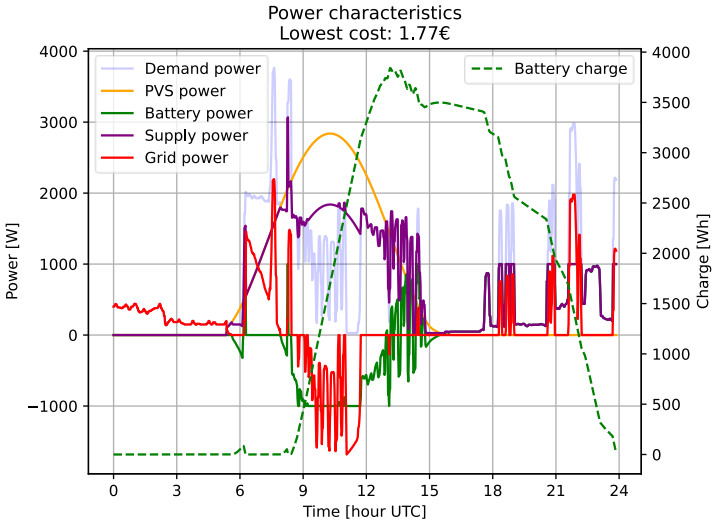

Figure 24: Power characteristics for best result of system with battery

In conclusion for the system with a battery "true" power matching cannot be observed. It rather seems of interest that the panel orientations are adapted to obtain the most power during the early part of the day to cover demands in the evening.

3.2.2. Future Scenarios Run

The future scenario results for the system with battery are presented in this Chapter. Figure 25 shows the panel orientations for the four defined scenarios. The plots show larger spreads than previous results for this system but there is no trend visible for orientation ranges different from those determined in the previous Section.

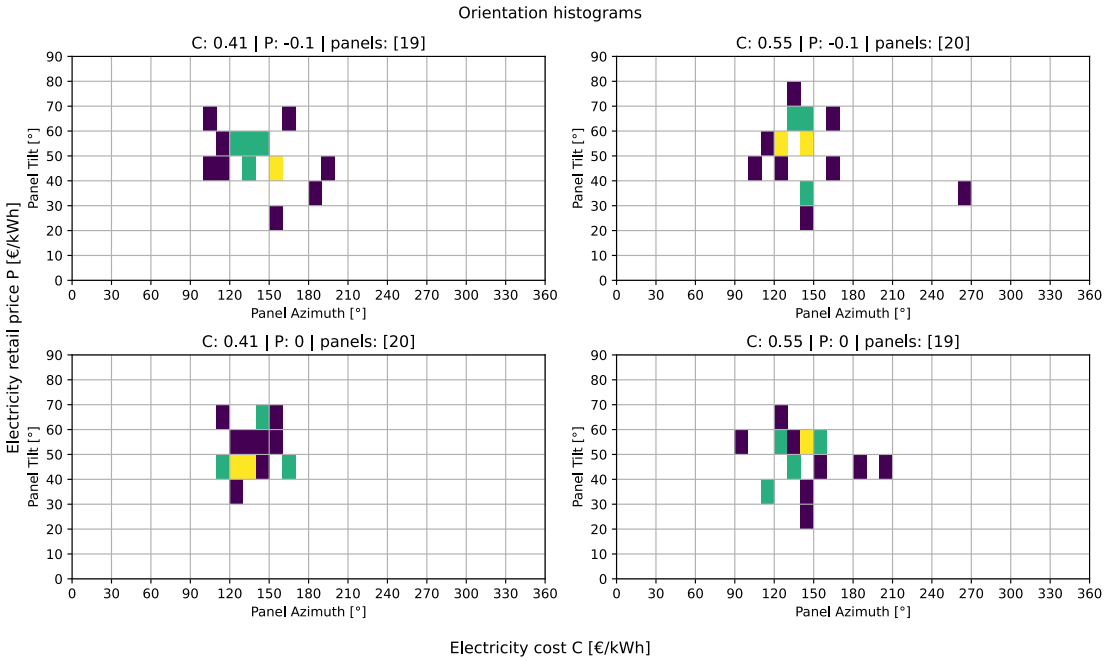

Figure 25: Panel orientations for different electricity costs and feed-in tariffs for system with battery.

The number of used panels do not change much either. Additionally, there is no bi-modality visible, meaning most of the panels face in one general direction. This also shows in the characteristics visualized in Figure 26. Here the overall result looks very much similar to the previous results with the current cost and feed-in tariff.

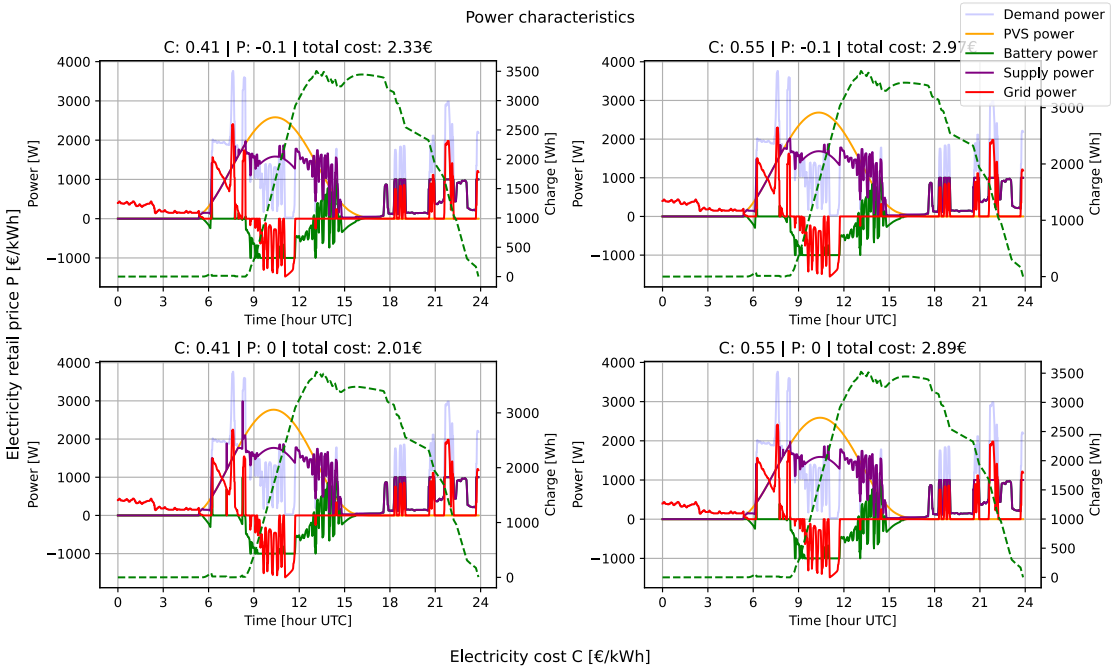

Figure 26: Power characteristics for different electricity costs and feed-in tariffs for system with battery.

For this system with a battery even the maximum power has hardly changed compared to the results in the previous chapter. This indicates that a PVS with a battery is more resilient against changes in electricity costs or feed-in tariff. It is sensible that this is the case as the edge case for this system would be that no power is needed from external sources and the system is self-sufficient.

4. Conclusion

Although the hypothesis in the introduction could not be confirmed in a sense that the production characteristic of photovoltaic power supplies was matched to a demand characteristic it could be demonstrated that there is some motivation to deviate from a purely southbound orientation of solar panels. This is especially true in cases where the electricity cost increases or even more so if the feed-in tariff becomes negative. A system with a battery is, however, more resilient against these effects.

The investigation could be expanded in many directions. For example the simulation could be continued for an entire year and the battery parameters could be considered as decision variables as well. Another possible direction of further analysis is the determination of a tipping point for electricity cost and feed-in tariffs after which a power matching is beneficial. Economically a simulation over the entire lifespan of a PVS could be investigated. Last the optimization could be run with more generations if more computational power is available.

References

[1] D. L. King, W. E. Boyson and J. A. Kratochvil, "Analysis of factors influencing the annual energy production of photovoltaic systems," in *Conference Record of the Twenty-Ninth IEEE Photovoltaic Specialists Conference*, New Orleans, LA, USA, 2002.

[2] A. Rohatgi, "WebPlotDigitizer," 2024. [Online]. Available: https://automeris.io. [Accessed 17 November 2024].

[3] "Astropy: A community Python package for astronomy," *Astronomy & Astrophysics*, vol. 558, p. A33, October 2013.

[4] "The Astropy Project: Building an Open-science Project and Status of the v2.0 Core Package," *Astronomical Journal*, vol. 156, p. 123, September 2018.

[5] "The Astropy Project: Sustaining and Growing a Community-oriented Open-source Project and the Latest Major Release (v5.0) of the Core Package," *Astrophysical Journal*, vol. 935, p. 167, August 2022.

[6] J. M. Palmer, "Kirt Witte's SCAD website," [Online]. Available: https://employeepages.scad.edu/~kwitte/documents/Photometry_FAQ.PDF. [Accessed 11 November 2024].

[7] University Corporation for Atmospheric Research, „The Troposphere," 2009. [Online]. Available: https://scied.ucar.edu/learning-zone/atmosphere/troposphere. [Zugriff am 17 November 2024].

[8] Statistisches Bundesamt (Destatis), "Erdgas- und Stromdurchschnittspreise," 2024. [Online]. Available: https://www.destatis.de/DE/Themen/Wirtschaft/Preise/Erdgas-Strom-DurchschnittsPreise/_inhalt.html. [Accessed 18 November 2024].

[9] Bundesnetzagentur, "EEG-Förderung und -Fördersätze," 2024. [Online]. Available: https://www.bundesnetzagentur.de/DE/Fachthemen/ElektrizitaetundGas/ErneuerbareEnergien/EEG_Foerderung/start.html. [Accessed 18 November 2024].

[10] M. Jónsson, *GA_Module_v6*, Reykjavík, 2024.

[11] Statistisches Bundesamt (Destatis), "Statistischer Bericht - Daten zur Energiepreisentwicklung - September 2024," 31 October 2024. [Online]. Available: https://www.destatis.de/DE/Themen/Wirtschaft/Preise/Publikationen/Energiepreise/statistischer-bericht-energiepreisentwicklung-5619001.html?nn=214072. [Accessed 19 November 2024].